AD-A160 476 HANDLING-QUALITIES INVESTIGATION OF CONVENTIONAL HELICOPTER DIRECTIONAL CONTROL CHARACTERISTICS(U) NATIONAL AERONAUTICS AND SPACE ADMINISTRATION MOFFETT FIELD C.. C C BIVENS 1985 1/1

UNCLASSIFIED F/G 1/3 NL

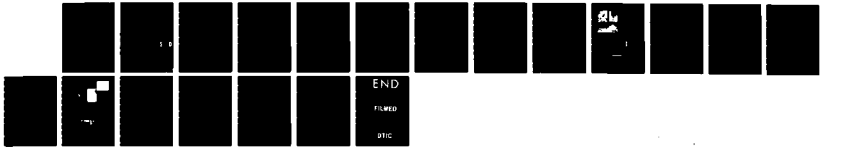

END

FILMED

DTIC

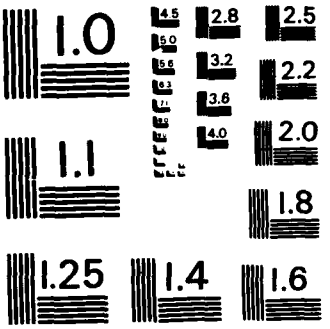

HANDLING-QUALITIES INVESTIGATION OF CONVENTIONAL HELICOPTER DIRECTIONAL CONTROL CHARACTERISTICS

Courtland C. Bivens
Aeroflightdynamics Directorate
Army Aviation Research and Technology Activity (ARTA)
Ames Research Center
Moffett Field, California

To be presented at the AIAA Guidance and Control Conference, Snowmass Conference Center, Snowmass, CO, August 19-21, 1985

HANDLING-QUALITIES INVESTIGATION OF CONVENTIONAL HELICOPTER DIRECTIONAL CONTROL CHARACTERISTICS

Courtland C. Bivens*
Aeromechanics Laboratory, U.S. Army Research and Technology Laboratories (AVSCOM)
Ames Research Center, Moffett Field, California

Abstract

A piloted simulation was conducted to investigate the directional-axis handling qualities of a conventional single-main-rotor/tail-rotor helicopter during the performance of low-speed (≤40 knots) tasks. The objectives of the experiment were to attempt to model the first-order effects that contribute to the loss of tail-rotor control that has been experienced by pilots of the OH-58 series aircraft, and to investigate handling-qualities parameters that reduce or eliminate tail-rotor-control problems in the context of the given test conditions. The aircraft configuration variables investigated were yaw damping (N_r), tail-rotor sensitivity (N_{δ_p}), and directional, or weathercock, stability (N_v). Two types of yaw stability and control augmentation systems were implemented, and an engine model was included to capture the effects of rotor angular speed variations on the total yawing moment, heave-axis force, and tail-rotor thrust capability. Five pilots evaluated 10 generic tail-rotor configurations in varied wind conditions while maneuvering through a nap-of-the-Earth (NOE) corridor terminating in a confined area at a hover. These evaluations were conducted on NASA Ames Research Center's vertical motion simulator; a visual system furnished the pilot with a four-window display of the NOE visual flight scene. A relatively simple tail-rotor model predicts the reductions in yaw damping and control power at certain relative wind azimuth angles which contribute to a loss of directional control. The loss of directional control occurred only for tail winds and quartering tail-winds greater than 20 knots for the specified flight task. For wind speeds greater than 20 knots, configurations with larger values of yaw damping were less susceptible to a loss of directional control; for winds greater than 30 knots, lower values of weathercock stability also had a beneficial effect. Finally, the effects of the particular engine model used in the simulation neither induced nor aggravated, in a substantial way, the conditions that led to loss of tail-rotor control over the range of variables investigated.

Nomenclature

AGL	= above ground level
AHIP	= Army Helicopter Improvement Program
C_g	= torque-to-power turbine, ft·lb
CHPR	= Cooper-Harper pilot ratings
$I_{E\&R}$	= combined power-turbine/rotor inertia, slug·ft^2
L_v	= scale length for v_g, ft
m	= mass
N_g	= gas generator speed, %
N_r	= yaw damping, sec^{-1}
N_v	= weathercock stability, rad/ft·sec
NOE	= nap of the Earth
N_{δ_p}	= yaw sensitivity due to pedal input, rad·sec^{-2}·in.$^{-1}$
Q_r	= torque required, ft·lb
Q_s	= torque supplied, ft·lb
rpm	= revolutions per minute
s	= Laplace operator
U	= aircraft velocity, ft/sec
U_o	= wind speed, ft/sec
v	= airspeed along y-body axis, ft/sec
v_g	= gust disturbance velocity along y-axis, ft/sec
Y_v	= side force per unit lateral velocity · 1/m, sec^{-1}
Y_r	= side force due to yaw velocity · 1/m, ft/(rad-sec)
Y_{δ_p}	= side force due to pedal control input · 1/m, (ft/sec^2)/in.
δ_p	= pedal movement, positive-right, in.
δ_c	= collective movement, in.

* Aerospace Engineer.

θ_{TR} = tail rotor pitch, deg

τ = system time constant = $1/N_r$, sec

$\Phi_{v_g}(\Omega)$ = spectrum for v_g

ψ_o = aircraft heading out of the wind direction, deg

$\dot{\psi}$ = yaw rate, deg/sec

$\ddot{\psi}$ = yaw acceleration, deg/sec^2

Ω = spatial (reduced frequency), rad/ft

Ω_o = rotor rpm

$\dot{\Omega}$ = rotor acceleration, rad/sec^2

Introduction

Current helicopter directional-control systems can, in certain low-speed flight conditions, be subjected to situations that severely affect the capability of the directional control device to provide the yawing moment required to trim, to counteract the effects of wind and turbulence, and to maneuver. Typical low-speed problems encountered by conventional helicopters utilizing a tail rotor for directional control include inadequate directional control when hovering in quartering tail-winds; large fluctuations in tail-rotor thrust as a result of quartering winds and nonsteady turbulence conditions; and loss of directional control effectiveness in low-speed translational and maneuvering flight with resultant uncontrollable spins. U.S. Army OH-58 series helicopters have encountered such problems[1,2] and have received considerable attention because of the number of aircraft that have been lost as a result of uncontrollable spins (Fig. 1). The following illustrates the sequence of events of the well-known, but not thoroughly understood problem.

> The OH-58C was assigned a mission which required flight at low level, going from point to point. The estimated gross weight was 3,000 pounds; pressure altitude: plus 1,390 feet; free air temperature: plus 30 degrees centigrade; wind: estimated from the southeast at 20 knots. Upon approaching the start point, the aircraft was slowed to less than 50 knots awaiting clearance to continue. The pilot initiated a right hand turn for entry into holding while still slowing. The holding turn was continued after completion of the first 360-degree turn at which time the tail seemed to weathervane into the wind and the aircraft made an almost 180 degree spin in the air around the mast. The pilot pushed in left pedal, added a little forward cyclic and added a small amount of power trying to gain a little forward airspeed. This seemed to aggravate the situation and the aircraft began a fast rate of spin to the right. Left pedal didn't seem to do anything. By this time, the aircraft had experienced 8 to 10 360-degree turns and was about 75 feet above the trees. With no place for a forced landing and not enough control over the aircraft to get to any landing area, the pilot made the decision to hold the collective pitch in place. The main rotor system began to bleed off and cyclic control was lost as the aircraft entered the trees. (Ref. 1)

In the absence of winds and turbulence for a given main-rotor torque setting (steady flight condition), there is a certain level of static tail-rotor thrust required to prevent the helicopter from yawing either left or right. This is known as tail-rotor trim thrust (Fig. 2). However, sufficient additional control power must be provided to regulate against winds and turbulence, and to maneuver the aircraft as dictated by mission requirements. The required tail-rotor thrust in low-speed flight is influenced by the wind speed and wind directions relative to the tail rotor.[3]

The available thrust of the tail rotor is also dependent on rotor rpm and hence on the engine-governing-system response characteristics.[1] For large transient rotor angular speed droops, owing to a poor governing system, the ability of the tail rotor to counteract main-rotor torque is decreased very significantly. In the case of the OH-58, a rotor speed droop of 3% will decrease the tail-rotor thrust by 9% (Fig. 3). The OH-58 exhibits very low values of directional damping[1]; it also exhibits a relatively high weathercock stability relative to that of other aircraft for speeds ≤40 knots (Ref. 1). By looking at the approximate open-loop transfer function for yaw-rate response owing to lateral gust near hover,

$$\frac{\dot{\psi}}{v_g} \simeq \frac{N_v}{s - N_r} \qquad (1)$$

it can be illustrated (Fig. 4) that for lower values of yaw damping and higher values of weathercock stability, the resulting yaw-rate response owing to v_g will be larger and possess a larger system settling-time constant, τ. The resulting tendency, if the pilot does not exert tight closed-loop control (compensate for larger τ), is for high yaw rates to be generated wherein the pilot may not have adequate remaining control power to arrest the resulting yaw rate. Accordingly, the experiment described in this paper

investigated these factors and the design parameters that could be used to reduce or eliminate tail-rotor control problems within the scope of an operational environment.

Experimental Design

Variables

The transfer function relating yaw rate to rudder input for translational flight is[4]

$$\frac{\dot{\psi}}{\delta_p}(s) = \frac{N_{\delta_p} s - Y_v \cdot N_{\delta_p} + Y_{\delta_p} \cdot N_v}{s^2 - (N_r + Y_v)s + (N_r Y_v - Y_r N_v) + UN_v} \qquad (2)$$

If the aircraft is in hovering flight, the above equation becomes[5]

$$\frac{\dot{\psi}}{\delta_p}(s) \cong \frac{N_{\delta_p} s}{s^2 - N_r s + U_o N_v \cos \psi_o} \qquad (3)$$

For low speeds (≤40 knots), the hover approximation can be used since these speeds are typical of those used for NOE flight. Hence, for typical NOE airspeeds and a given set of wind conditions, the dominant contributors to directional stability and control characteristics are N_{δ_p}, N_r, and N_v.

For this experiment, the weathercock stability (N_v) and yaw angular rate damping (N_r) were examined as independent variables. Yaw-axis control sensitivity (N_{δ_p}) was dependent on the value of N_r to attempt to maintain a near-constant steady-state yaw rate. Table 1 depicts the combinations of the various parameters that composed each test configuration. The mathematically derived values of the OH-58 for airspeeds ≤40 knots are also shown in Table 1 relative to the test configurations.

Simulation Model Description

The aircraft equations of motion were represented by the full set of nonlinear gravitational and inertial terms of the equations. The aerodynamic forces and moments were represented by reference values and first-order terms of a Taylor-series expansion about a reference trajectory defined as a function of the total airspeed.[5] Values of the trim, stability, and control parameters for the basic Scout aircraft were obtained from a generic, nonlinear mathematical total-force-and-moment model of a single-main-rotor helicopter (ARMCOP), using input source data from the Bell model-406 Army Helicopter Improvement Program (AHIP).[6] The ARMCOP tail rotor is assumed to be a two-bladed teetering rotor; tail-rotor flapping, the vortex ring state dynamics, and adverse fin flow were not modeled. To represent primary nonlinear tail-rotor effects, N_r and N_{δ_p} were varied as a function of magnitude and as a direction of the relative wind; this technique produced results that compared very favorably with data reported in Refs. 7 and 8 (Figs. 5 and 6).

An engine model was included in the simulation to take into account the effects of variations in rotor rpm on the total yawing moment and heave-axis force. The engine model included a representation of an electronic fuel control system; for a 1-in. change in collective, the rotor rpm exhibited a maximum transient droop of less than 1% (Fig. 7). It can be seen from Fig. 7 that this 1% transient droop only changed the trim pedal required from 0.2 in. to 0.5 in. Because of the scope and time limitation of the experiment, the droop characteristics were not parametrically varied to investigate fully power-droop effects on the spin phenomena.[1,2]

The yaw-axis stability and control augmentation systems (SCAS) included two provisions for hover and low-speed (≤40 knots). The actual details of implementation of these systems for this simulation are discussed in Ref. 5. The basic yaw SCAS comprised washed-out yaw-rate damping and control quickening (Fig. 8). The rate-command, heading-hold included integral plus rate feedback and an integral-plus-proportional feed-forward to provide steady-state acceleration (Fig. 8). A dead zone was included in the integral feed-forward paths to prevent drift caused by the integration of inadvertent pilot control inputs.

The pitch and roll axes were augmented with inertial velocity command systems, and the heave axis consisted of a rate-command altitude-hold system. This was done to maintain good flying qualities in the pitch, roll, and heave axes so that those axes would not become dominant factors affecting pilot opinion.

Since the wind and turbulence conditions are significant factors in setting up conditions that are conducive to the loss of tail-rotor control effectiveness, it was necessary to include these effects in the simulation. To provide the effects of steady wind and wind shear, the magnitude of the steady wind was specified at two altitudes: 20 and 200 ft AGL. Linear interpolation was used to determine mean wind speed between these altitudes. Beyond these altitude extremes, the mean wind speed remains constant. The wind was from 360°. This direction was selected so that the aircraft, while traversing the course would have to make left and right downwind turns. References 1-3 make it clear that this tail-wind condition is the one in which the problem usually occurs. The turbulence model used was of the Dryden form of the spectra for turbulence

velocities. For the disturbance velocity along the y-axis, this consisted of[11]

$$\Phi_{v_g}(\Omega) = \sigma_v^2 \frac{L_v}{\pi} \frac{1 + 3(L_v\Omega)^2}{[1 + (L_v\Omega)^2]^2}$$

Turbulence intensity spectra for the x-axis and z-axis velocities were also computed. Further details of turbulence spectra, and defined scale lengths are given in Refs. 5 and 9. The vertical turbulence intensity is specified as 10% of the mean wind speed at 20 ft AGL. The ratio of the horizontal turbulence intensities to the vertical intensity varies as a function of altitude from a value of 1 at 1,000 ft to a value of 2 at the surface. The wind and turbulence conditions defined for this experiment are given in Table 2.

Facility and Cockpit Configuration

This piloted simulation was conducted on the Ames Research Center Six-Degree-of-Freedom Vertical Motion Simulator (Fig. 9). A four-window computer-generated-image (CGI) system provided the outside visual display scene. Figure 10 shows the view of each of the four CGI windows superimposed on the pilot's field of view in a typical Scout helicopter. The scene shown is part of the NOE canyon course. The rocks and trees on the sides of the canyon wall were used to provide height and attitude cues. The patterning on the canyon walls and floor provided the relative translational motion cues.

A head-up-display/panel-mounted-display (HUD/PMD) was provided in the cockpit to compensate for the restricted field of view and the low level of detail of the simulator visual system. The symbols that were presented to the pilot are illustrated in Fig. 11.

A Sigma-8 computer generated the simulator mathematical model, and a digital PDP 11/40 computer drove both the Evans and Sutherland HUD and a 9-in. Kratos PMD. A conventional helicopter control arrangement similar to the AHIP was used with artificial force-feed loaders that drove a cyclic stick, a collective stick, and pedals (Fig. 12). The control system characteristics are listed in Table 3. A sound system provided realistic helicopter aural cues driven by parameters from the mathematical model used in the simulation.

Experiment

In this experiment the task assigned to the pilot included control of the aircraft and associated functions, but it did not include tasks that were indirectly related to control of the aircraft such as navigation and communications. The overall mission called for Scout operations in an NOE environment conducive to loss of tail-rotor control. The mission profile consisted of two task segments representative of a typical Scout mission conducted during the day,[10] specifically, NOE flight and deceleration to a hover.

The profile began at the start point (Fig. 13) with the aircraft at 50 ft, heading 225°, and 40 knots. After negotiating the canyon course at or below 50 ft above ground level (AGL), a deceleration maneuver was performed with the aircraft coming to a hover (10 ft AGL) in the center of the hover area pointing 270°. At the conclusion of the run, a Cooper-Harper pilot rating[11] was assigned to each task segment, and general pilot comments regarding the yaw axis handling qualities were elicited. Aircraft state and task performance data were also recorded.

Five pilots served as evaluation pilots for the experiment:

1) Pilot 1: Army experimental test pilot with 3,400 flight hours, 2,200 of which were in rotary-wing aircraft; 100 hr NOE experience.

2) Pilot 2: Army experimental test pilot with 3,800 flight hours, 1,700 of which were in rotary-wing aircraft; 100 hr NOE experience.

3) Pilot 3: Civilian experimental test pilot with 5,100 flight hours, 2,900 of which were in rotary-wing aircraft; 500 hr NOE experience.

4) Pilot 4: Army experimental test pilot with 4,700 flight hours, 3,600 of which were in rotary-wing aircraft; 75 hr NOE experience.

5) Pilot 5: Army-pilot/engineer with 1,100 flight hours, 1,000 of which were in rotary-wing aircraft; 400 hr NOE experience.

Results

In investigating the loss of tail-rotor effectiveness, 47 data runs were obtained. The moderate and strong wind conditions were evaluated by one engineer/pilot, and the remaining configurations were flown by four test pilots. The resulting averaged Cooper-Harper ratings are presented in Table 4.

By modeling the first-order effects of N_r, N_v, and N_{δ_p} for different wind conditions and azimuths, it was possible to induce a right-spin that was characteristic of that encountered during loss of tail-rotor control effectiveness in OH-58 series aircraft. These results do not imply that these are the only variables or circumstances involved in the loss of tail-rotor control, but the investigation of these factors laid more groundwork for further research.

For yaw damping levels of $|N_r| \leq 1.0$ with moderate or strong wind conditions, control of the aircraft was lost or the aircraft was flown into the surrounding terrain while the pilot was attempting to initiate a recovery. All of the

loss of control incidents occurred during the 110° right turn, where a right spin was encountered.

No loss of directional control was encountered in the left 65° turn; however, pedal margin limits were reached in certain instances. The left turn required yawing the tail of the aircraft into the relative wind. Conversely, the right turn required the tail to yaw out of the direction of the wind. Pilot comments indicate that the very sharp right turn, which took coordinated roll- and yaw-control inputs, required initially a higher than normal yaw-control input. This commanded yawing moment, combined with the yawing moment caused by the high weathercock stability, resulted in excessive yaw rates to the right for low values of yaw damping. The tail rotor would then lose some effectiveness as a result of receiving a relative wind coming from ψ_o angles of 30° to 90° (Fig. 4). Because of the severity of the wind, the yaw-rate commanded by the pilot, the yaw damping of the aircraft, and the effective reduction in yaw-control power, the spin was induced. Figure 14 shows some of the aircraft dynamic states and control positions during a typical loss-of-control case (N_r = -0.5, N_v = 0.01, N_{δ_p} = 0.5).

Additional pilot comments indicated that if the loss of control had occurred at a higher altitude (≥200 ft) recovery might have been possible by maintaining full left pedal and forward cyclic. Adding additional collective during the spin tended to aggravate the condition by increasing the rotor torque effect. When the pilots attempted to decrease the effect of main-rotor torque by decreasing the collective, the result was usually ground or tree contact during the attempted recovery.

While performing the left turn, control was not lost, even though control-power margins may have been reached. With reference to Fig. 4, a left turn would generate a relative wind on the tail rotor from ψ_o angles of 270° to 330°. In this area, damping is adequate but increased thrust is required. Pilot comments also alluded to the fact that since the left turn was not as severe as the right turn, smaller values of yaw rate were utilized. This left yaw rate was also diminished by the weathercock stability of the aircraft. In effect, this caused the pilot to increase the left pedal in order to attempt to line up the nose of the aircraft with the line of flight. On occasion, the pilots would continue adding pedal until the margin was reached. Since no large yaw rates were encountered, the pilot would be in a near-steady-state condition with full left pedal. The pilots commented that this was not desirable, but that they could compensate for this condition by adding left cyclic and flying with the nose of the aircraft out of trim to the right. This procedure is also illustrated in Fig. 13.

By decreasing the value of the aircraft directional gust sensitivity parameter (N_v) from 0.02 to 0.01 in strong winds, it was observed that pilot ratings improved for yaw damping values of -4.0 and -6.0; for damping values of -0.5 and -1.0 in moderate and strong winds, aircraft control was lost for both values of gust sensitivity. For light winds, no degradation in pilot rating with increasing gust sensitivity was evident ($N_v \cdot v_g$ is insignificant).

Because of the excellence of the engine-governing system, the main-rotor rpm changed less than ±1.0%. Even though the rpm effects were coupled to the aircraft yawing moment, a 1% droop in rpm required only a 0.3 in. change in required left pedal (δ_p). Pilot comments further indicated that rpm control was not a major factor inducing or aggravating the loss of yaw-control effectiveness in this experiment. This result does not imply that poor rpm control is not a factor in the tail-rotor loss of control, but that with a very good governor, rpm control is eliminated as a factor.

By adding a yaw SCAS or rate-command heading-hold augmentation to a configuration with low yaw damping (N_r = -1.0), the averaged pilot ratings improved. The pilots commented that the nose of the aircraft had less of a tendency to oscillate, and that it was very easy to modulate the yaw rates within an acceptable margin even with the addition of wind and turbulence and severe right-turn maneuvering.

Conclusions and Recommendations

A piloted simulator investigation of the directional stability and control characteristics of selected single-main-rotor/tail-rotor configurations under various wind and turbulence conditions was conducted on the six-degree-of-freedom vertical motion simulator at Ames Research Center. The objectives of the experiment were to attempt to model the first-order effects that contribute to the loss of tail-rotor control experienced by the OH-58 series aircraft, and to investigate handling-qualities parameters that reduce or eliminate tail-rotor control problems in the context of the given test conditions.

The following conclusions are based on the pilot evaluations and quantitative data obtained.

1) A relatively simple tail-rotor model predicts the reductions in yaw damping and control power at certain relative wind azimuth angles which contribute to a loss of directional control.

2) Loss of directional control occurred only for tail winds and quartering tail-winds greater than 20 knots for the specified flight task.

3) For wind speeds greater than 20 knots, configurations with larger values of yaw damping ($|N_r| \geq 1.0$ sec^{-1}) were less susceptible to a loss

of directional control; for winds greater than 30 knots, lower values of weathercock stability (N_v < 0.01) also had a beneficial effect.

4) The effects of this particular engine model did not significantly induce or aggravate the conditions that result in the loss of tail-rotor-control.

5) For additional understanding of the spin phenomenon, it is recommended that the following pilot simulations be conducted:

- Tests of different types of yaw SCAS configurations at higher wind conditions

- Tests of configurations with substantially degraded engine-governing systems to study the significance of main-rotor/tail-rotor rpm droop

- Investigations with different task constraints (wider or tighter right turns)

- Tests with various additional environmental conditions

6) It is recommended that the effects of adverse fin force and tail-rotor vortex ring state be included in the mathematical model.

References

[1]Merritt, Donald E. and Cioffi, Charles C., "OH-58 Tail Rotor Control Power," U.S. Army Aviation Digest, Mar. 1983.

[2]"OH-58 Tail-Rotor Stall," U.S. Army Aviation Digest, Nov. 1978.

[3]Snellen, David M., "OH-58 Loss of Tail Rotor Effectiveness, Why It occurs," U.S. Army Aviation Digest, Sept. 1984.

[4]Gould, D. G. and Daw, D. F., "A Flight Investigation of the Effects of Weathercock Stability on V/STOL Aircraft Directional Handling Qualities," NRCLR-400, National Research Council of Canada, May 1964.

[5]Aiken, E. W., "A Mathematical Representation of an Advanced Helicopter for Piloted Simulator Investigations of Control System and Display Variations," AVRADCOM TM 80-A-2, June 1980.

[6]Talbot, P. D., Decker, W. A., Tinling, B. E., and Chen, R. T., "A Mathematical Model of a Single-Main-Rotor Helicopter for Piloted Simulation," NASA TM-84281, 1982.

[7]Blake, Bruce B. and Hooper, D., "Wind Tunnel Investigation into the Directional Control Characteristics of an OH-58 Helicopter," Applied Technology Laboratory, U.S. Army Aviation Systems Command (AVSCOM), Ft. Eustis, Va., Apr. 1983.

[8]Marshall, Roy, "OH-58C Vertical Fin Blockage Evaluation," U.S. Army Aviation Experimental Flight Activity Project 83-03, 6 Oct. 1983.

[9]"Military Specification: Flying Qualities of Piloted Airplanes," MIL-F-8785C, 5 Nov. 1980.

[10]"Aircrew Training Manual--Observation Helicopter," Training Circular No. 1-136, U.S. Army Aviation Center, Jan. 1981.

[11]Cooper, G. E. and Harper, R. P., "The Use of Pilot Rating in the Evaluation of Aircraft Handling Qualities," NASA TN D-5153, 1969.

Table 1 Experimental parameters[a]

	① N_r, sec^{-1} / N_{δ_p}, $\frac{rad/sec^2}{in.}$	-0.5 / 0.5	-0.75 / 1.65	-1.0 / 0.75	-4 0 / 1 0	-6 0 / 1.65
N_v $\frac{rad/sec^2}{ft/sec}$	0.02	CONF 1	OH-58	CONF 2	CONF 3	CONF 4
	0.01	CONF 5		CONF 6	CONF 7	CONF 8

1 ZERO WIND VALUES OF N_r AND N_{δ_p}

Table 2 Simulated wind conditions

	20 ft (AGL)	200 ft (AGL)
LIGHT	19 knots	21 knots
MODERATE	21 knots	26 knots
STRONG	34 knots	45 knots

Table 3 Simulation vehicle control system characteristics

	COLLECTIVE SYSTEM	LONGITUDINAL CYCLIC SYSTEM	LATERAL CYCLIC SYSTEM	DIRECTIONAL SYSTEM
CONTROL TRAVEL	10.65 in.	10.66 in.	8.54 in.	6.50 in.
SWASHPLATE TRAVEL	1 FULL DOWN 17 FULL UP	11 FORWARD 11 AFT	6.0 LEFT 6.0 RIGHT	
ROTOR BLADE TRAVEL AT 0.75R	16	22	12	40
ROTOR GEARING	1.5 /in.	2.06 /in.	1.43 /in.	6.15 in.
CONTROL BREAKOUT FORCE (ZERO FRICTION)	2.0 lb	0.5 lb	0.5 lb	4.0 lb
CONTROL FORCE GRADIENT	0.0 lb/in.	1.05 lb/in.	0.68 lb/in.	3.5 lb/in.
LIMIT CONTROL FORCES	3.0 lb	6.1 lb	3.4 lb	15.0 lb

Table 4 Cooper-Harper ratings

N_v, rad/sec^2/ft/sec	N_r, sec^{-1}				
	-.5	-1.0	-4.0	-6.0	WIND
0.02		6.75(4[1])	5.0	4.75	LIGHT
	10	10	6	4	MODERATE
	10	10	10	8	STRONG
0.01	6.75	5.4	4.25	4.33	LIGHT
	10	10	5	3.5	MODERATE
	10	10	4	6	STRONG

1 YAW AUGMENTATION ADDED

☐ LOSS OF TAIL ROTOR CONTROL ENCOUNTERED

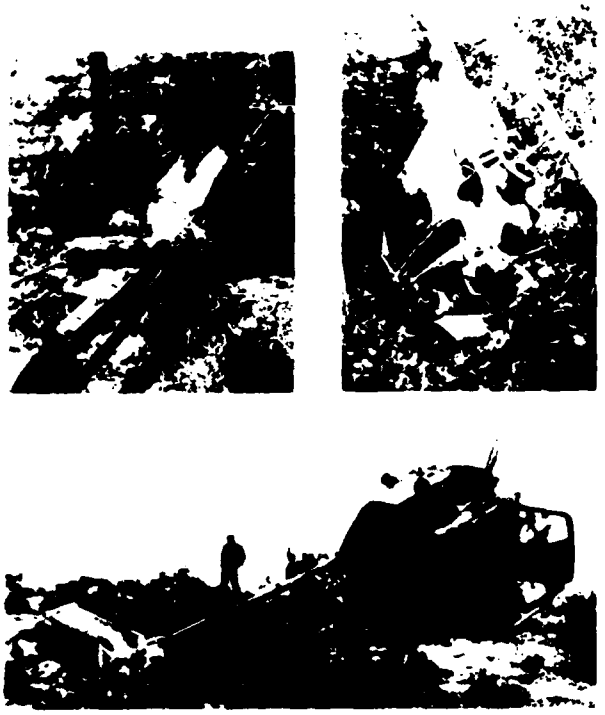

(Courtesy of U.S. Army Aviation Digest, March 1983)

Fig. 1 Accidents caused by loss of tail-rotor control authority.

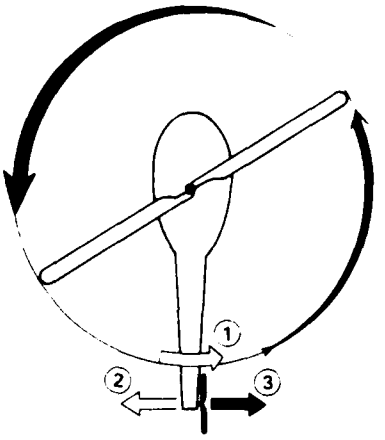

1. ROTATION DIRECTION OF ENGINE DRIVEN MAIN ROTOR
2. TORQUE EFFECT ROTATES FUSELAGE IN DIRECTION OPPOSITE TO MAIN ROTOR
3. TAIL ROTOR COUNTERACTS TORQUE EFFECT AND PROVIDES POSITIVE FUSELAGE HEADING CONTROL

Fig. 2 Tail-rotor trim thrust.

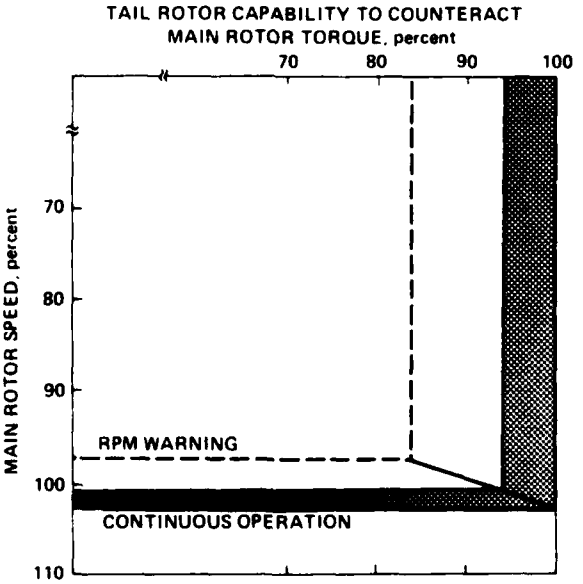

Fig. 3 OH-58A rotor speed effect on tail-rotor capability (from Ref. 1).

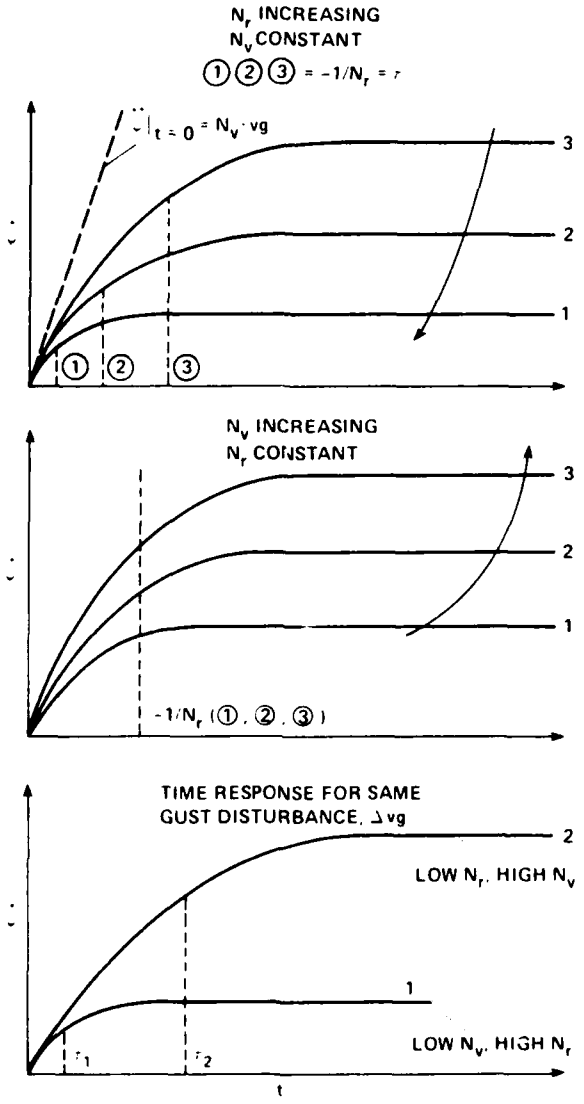

Fig. 4 Time response effects of N_r and N_v.

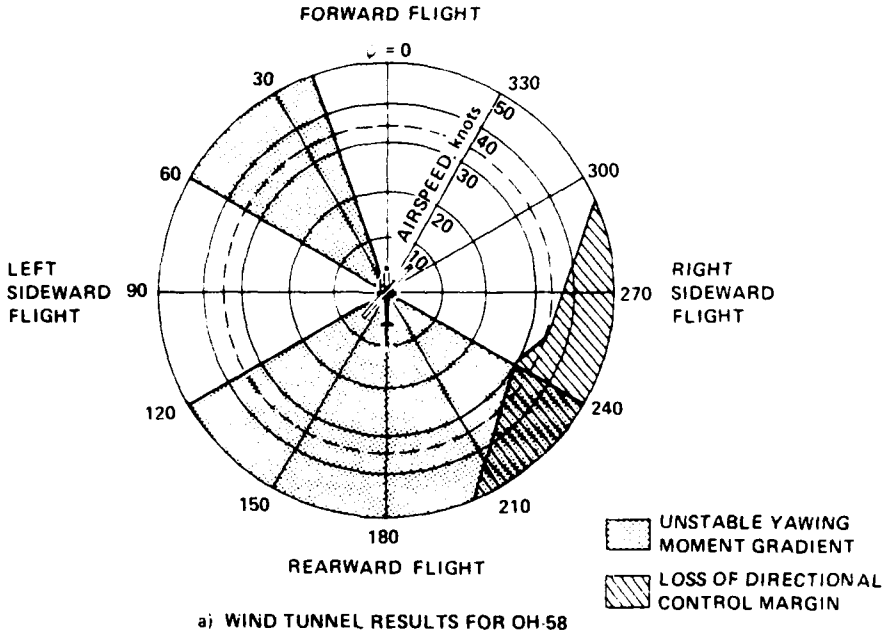

a) WIND TUNNEL RESULTS FOR OH-58

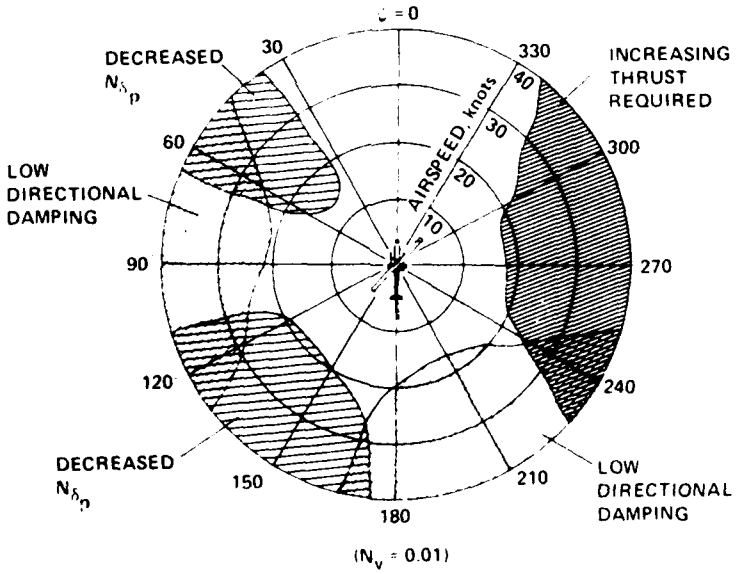

b) NONLINEAR MATHEMATICALLY MODELED DIRECTIONAL CONTROL CHARACTERISTICS

Fig. 5 Comparison of mathematically derived and wind tunnel results of Scout directional control characteristics.

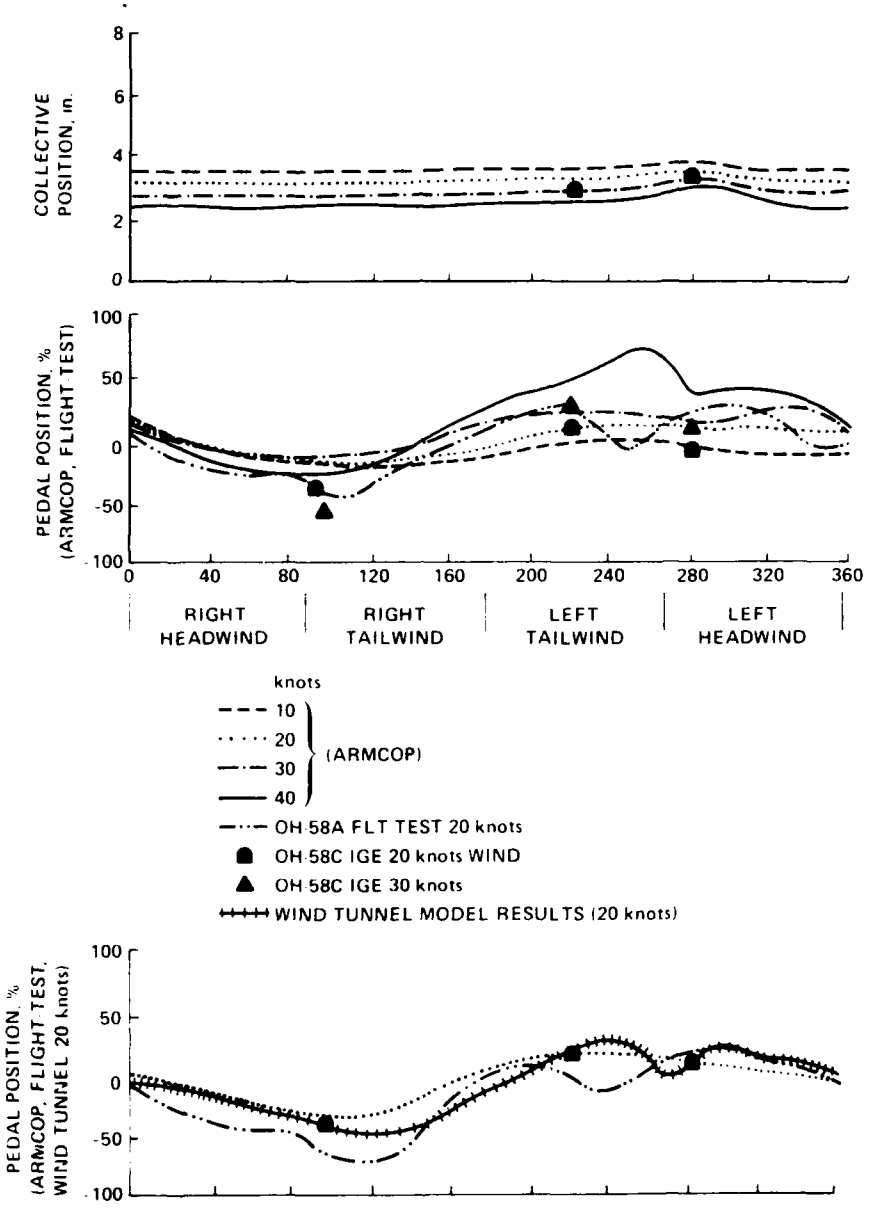

Fig. 6 Comparison of pedal and collective positions for ARMCOP, wind tunnel, and flight-test data (Refs. 7,8).

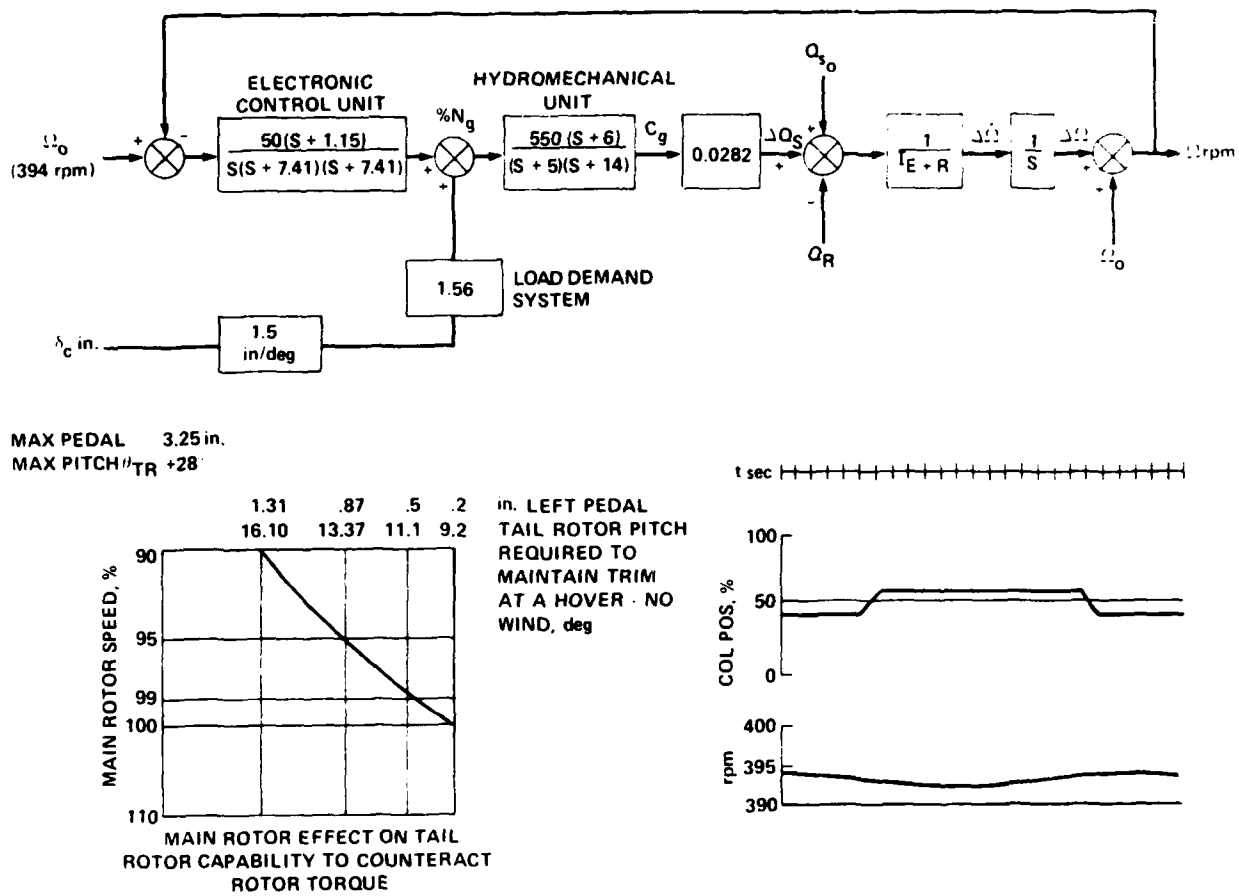

Fig. 7 Scout helicopter engine model effects on tail-rotor thrust.

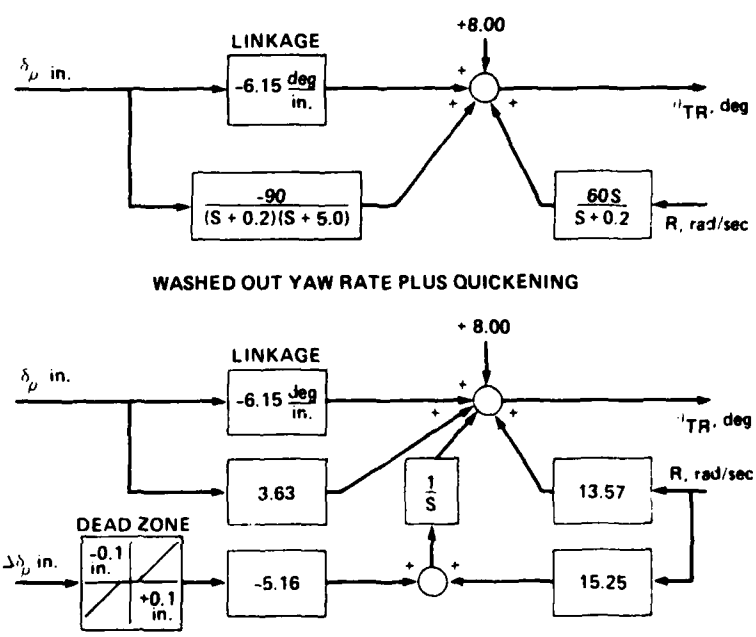

Fig. 8 Yaw axis augmentation schemes.

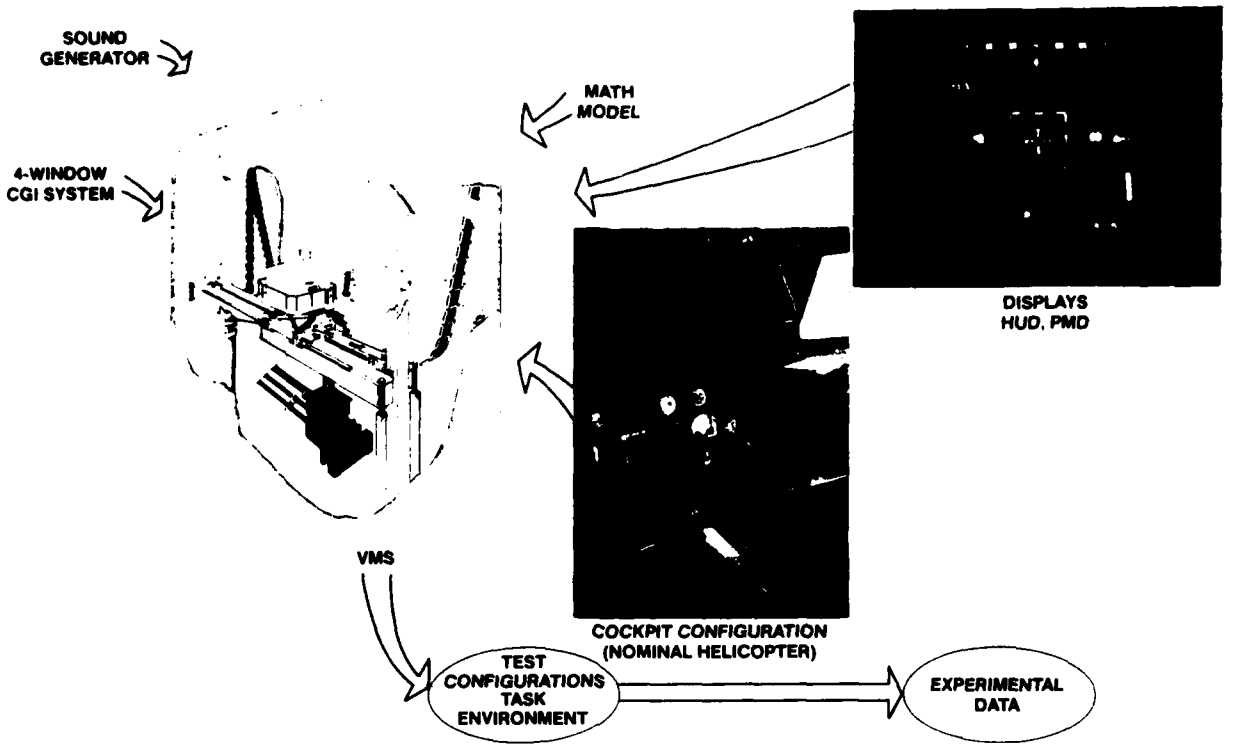

Fig. 9 Facility.

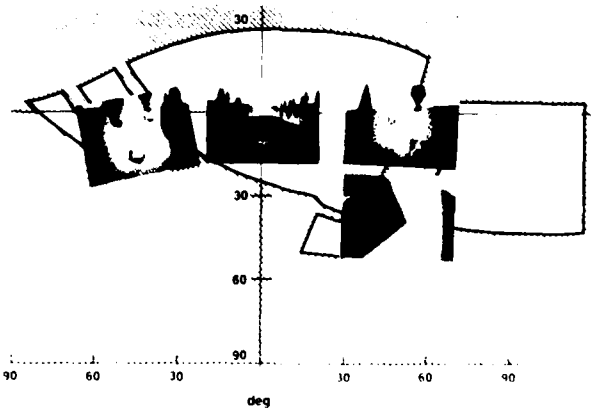

Fig. 10 Four window computer generated display of terrain scene.

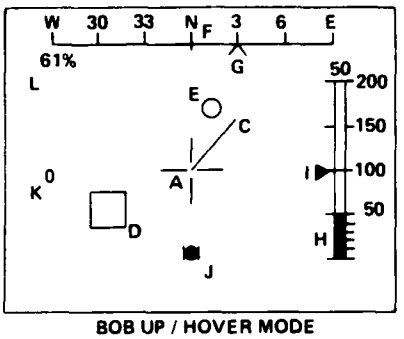

BOB UP / HOVER MODE

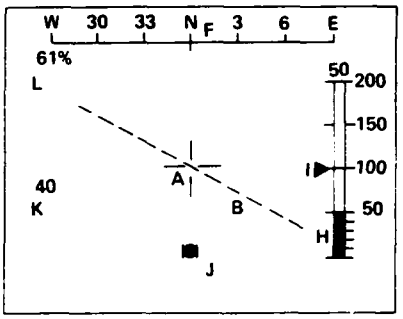

CRUISE / TRANSITION MODE

SYMBOL	INFORMATION
A. AIRCRAFT REFERENCE	FIXED REFERENCE FOR HORIZON LINE VELOCITY VECTOR, HOVER POSITION, CYCLIC DIRECTOR, AND FIRE CONTROL SYMBOLS
B. HORIZON LINE (CRUISE MODE ONLY)	PITCH AND ROLL ATTITUDE WITH RESPECT TO AIRCRAFT REFERENCE (INDICATING NOSE-UP PITCH AND LEFT ROLL)
C. VELOCITY VECTOR	HORIZONTAL DOPPLER VELOCITY COMPONENTS (INDICATING FORWARD AND RIGHT DRIFT VELOCITIES)
D. HOVER POSITION	DESIGNATED HOVER POSITION WITH RESPECT TO AIRCRAFT REFERENCE SYMBOL (INDICATING AIRCRAFT FORWARD AND TO RIGHT OF DESIRED HOVER POSITION)
E. CYCLIC DIRECTOR	CYCLIC STICK COMMAND WITH RESPECT TO HOVER POSITION SYMBOL (INDICATING AIRCRAFT FORWARD AND TO RIGHT OF DESIRED HOVER POSITION)
F. AIRCRAFT HEADING	MOVING TAPE INDICATION OF HEADING (INDICATING NORTH)
G. HEADING ERROR	HEADING AT TIME BOB-UP MODE SELECTED (INDICATING 030)
H. RADAR ALTITUDE	HEIGHT ABOVE GROUND LEVEL IN BOTH ANALOG AND DIGITAL FORM (INDICATING 50 ft)
I. RATE OF CLIMB	MOVING POINTER WITH FULL-SCALE DEFLECTION OF ± 1,000 ft/min (INDICATING 0 ft/min)
J. LATERAL ACCELERATION	INCLINOMETER INDICATION OF SIDE FORCE
K. AIRSPEED	DIGITAL READOUT IN knots
L. TORQUE	ENGINE TORQUE IN percent

Fig. 11 HUD/PMD symbols.

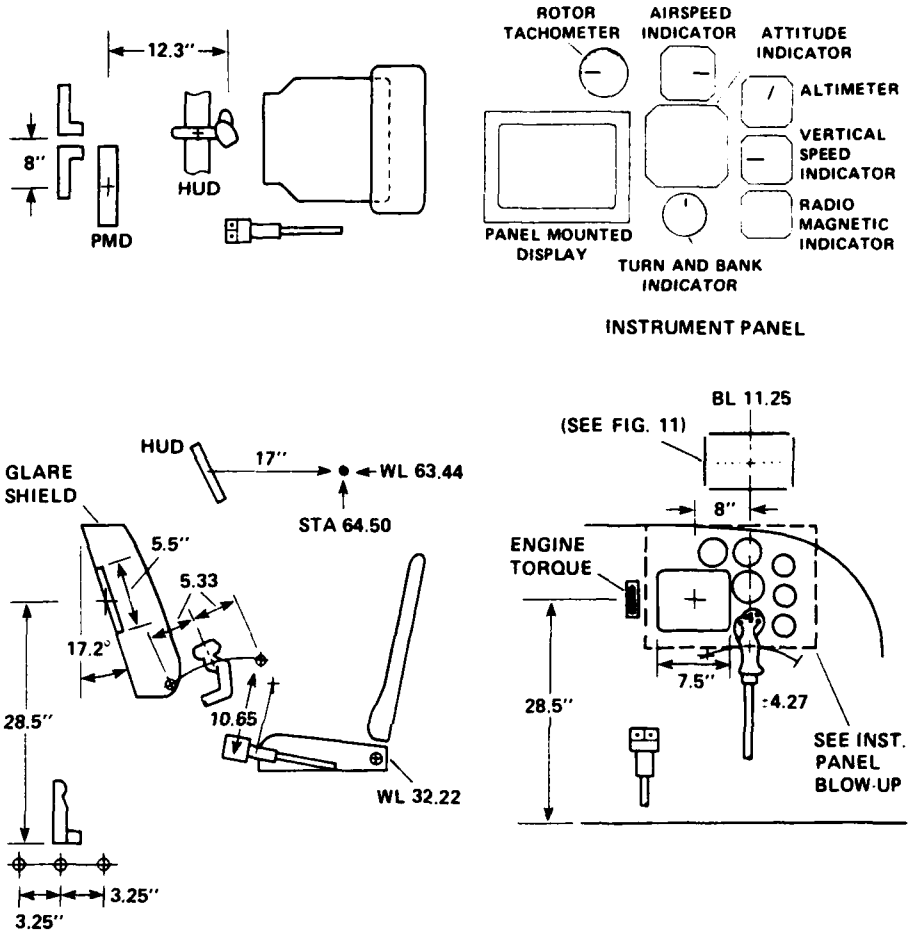

Fig. 12 Arrangement of cockpit.

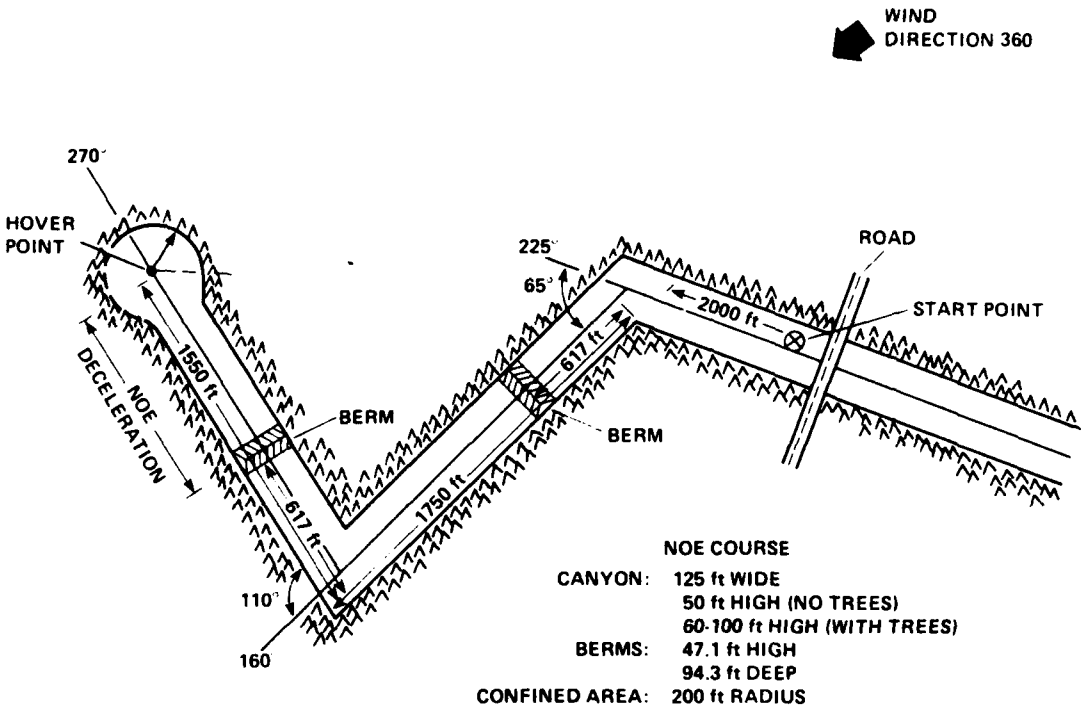

Fig. 13 NOE course.

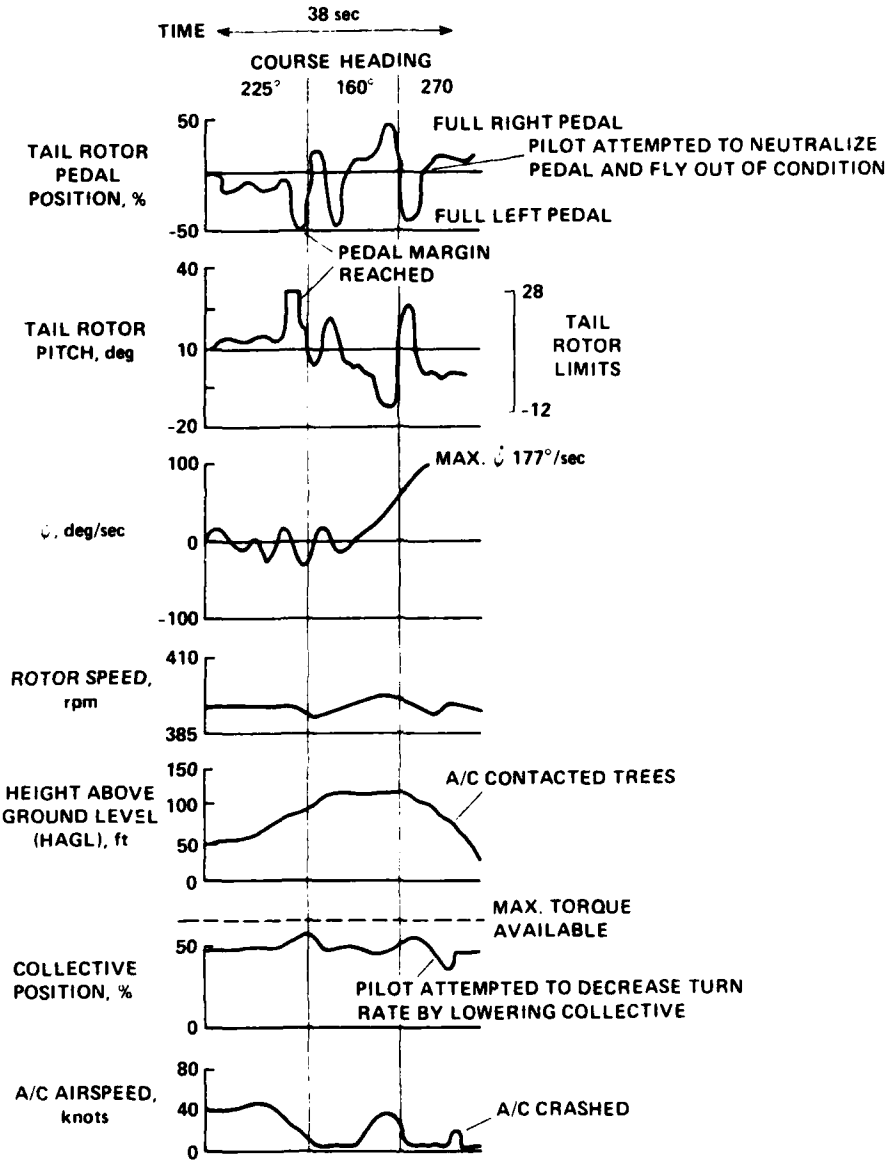

Fig. 14 Typical loss of tail-rotor control: N_r = -0.5, N_v = 0.01, N_{δ_p} = 0.5.

END

FILMED

12-85

DTIC